

29

30 **Keywords:** sexual dichromatism, dorsal frog colouration, ventral frog colouration, amphibian
31 sex reversal, XX male

32

33 **Abstract**

34 In species with sexual dichromatism, colouration can play an important role in intraspecific
35 communication and affect breeding success. Communication by visual signals during the
36 breeding season has been increasingly recognized to occur in anuran amphibians. However,
37 most studies of sexual dichromatism have focused on consistent differences between males and
38 females, and species with varying combinations of sexual genotypes and phenotypes have so
39 far been overlooked. We studied dorsal and ventral colouration of the agile frog (*Rana*
40 *dalmatina*), a species where genetically female (XX genotype) tadpoles experiencing warm
41 environmental temperatures tend to undergo sex reversal. In accordance with this laboratory-
42 based observation, phenotypic males with both XX and XY genotype occur in free-ranging
43 populations, but ‘XX males’ have reduced breeding success despite being fertile. We compared
44 different aspects of colouration between females, ‘XX males’ and ‘XY males’ to assess whether
45 there is sexual dichromatism between the phenotypic sexes, and whether ‘XX males’ differ
46 from ‘XY males’ in any of the measured parameters. We found that females differed from
47 phenotypic males in both dorsal and ventral colouration. These differences were also supported
48 by the frog vision model. Females showed a trend towards darker, more red-shifted dorsal and
49 throat coloration, and featured substantially more ventral pigmentation near the rostral tip of
50 the mouth relative to phenotypic males. Most females featured a red ventral pattern on the
51 anterior part of the trunk that almost never occurred in males. Interestingly, ‘XX males’ showed
52 a shift towards yellower average throat colouration relative to ‘XY males’; however, the
53 difference was small and not detectable under the frog vision model. Our results suggest that
54 agile frogs may rely on colouration for intraspecific communication during the breeding season,
55 similarly to other species in this genus, but visual cues are unlikely to mediate the recognition
56 of sex-reversed males.

57

58 **1. Introduction**

59 Sexual dichromatism often facilitates intraspecific communication, affects mate choice and
60 may also cause differential predation risk between the sexes (Hirschmann & Hödl, 2006; Bell
61 & Zamudio, 2012; Rojas, 2017; Höbel *et al.*, 2022; Rojas *et al.*, 2023). However, sexual
62 development in some systems is more complex than what simple differentiation between males
63 and females could describe. Certain environmental conditions can cause sex reversal during
64 early ontogeny in a variety of ectotherm vertebrate species (Baroiller & D’Cotta, 2001; Li *et*
65 *al.*, 2016; Nemesházi & Bókony, 2023), resulting in the development of opposite gonadal sex
66 to what is expected based on sex chromosomes. Thus, the phenotypic traits of sex-reversed
67 individuals may theoretically differ from those of their sex-concordant counterparts, potentially
68 resulting in differential fitness (Li *et al.*, 2016; Bókony *et al.*, 2021, 2025b; Nemesházi *et al.*,
69 2021; Wild *et al.*, 2023). Because their sex chromosomes correspond to one sex, whereas their
70 ontogenetic sexual development corresponds to the other, sex-reversed individuals may
71 resemble one sex in some traits and the other sex in other traits (Li *et al.*, 2016). In fish,
72 laboratory experiments have reported colouration differences between sex-reversed and
73 concordant individuals (Edmunds *et al.*, 2000). Although sex-reversal has so far been confirmed
74 in only a handful of amphibian and reptile species, indirect evidence suggests that it may be far
75 more widespread than currently recognized, and climate change may increase its frequency
76 worldwide (Geffroy & Wedekind, 2020; Whiteley *et al.*, 2021; Nemesházi & Bókony, 2025).
77 Yet, empirical data on the effects of sex reversal on visible phenotypes, physiology and
78 behaviour in the herpetofauna remain scarce (Li *et al.*, 2016; Bókony *et al.*, 2021, 2025b; Wild
79 *et al.*, 2023), and to our knowledge no study has assessed its effects on colouration in
80 amphibians or reptiles (but see Ujhegyi & Bókony, 2020, where a proportion of the studied
81 female toads were sex reversed).

82 The agile frog (*Rana dalmatina*) is an emerging model system for sex-reversal research
83 (Nemesházi *et al.*, 2020; Bókony *et al.*, 2021, 2025a; Mikó *et al.*, 2021; Ujszegi *et al.*, 2022).
84 In this amphibian, elevated environmental temperatures experienced during larval development
85 can induce female-to-male sex reversal (Ujszegi *et al.*, 2022). While females have XX sex-
86 chromosome genotype and sex-concordant males have XY genotype, sex-reversed males are
87 genotypic females (XX genotype) with male primary and secondary sexual characteristics
88 (Nemesházi *et al.*, 2020). In free-ranging agile frog populations, the proportion of sex-reversed
89 individuals among phenotypic males increases with anthropogenic land use (Nemesházi *et al.*,
90 2020). Effects of sex reversal on phenotypic traits other than growth and condition in early life
91 (Bókony *et al.*, 2021, 2025a; Mikó *et al.*, 2021; Ujszegi *et al.*, 2022) have received little

92 attention. Recent findings suggest that female agile frogs differentiate between sex-reversed
93 ‘XX males’ and concordant ‘XY males’ during mating, but the basis of this differentiation is
94 currently unknown (Bókony *et al.*, 2025b). Due to its fundamental role in both communication
95 and camouflage in amphibians (Rojas, 2017; Rojas *et al.*, 2023), studying colouration in agile
96 frogs may provide crucial information on the fitness-related consequences of sex reversal.

97 Both dorsal and ventral colouration differ between the sexes in several amphibian species (Todd
98 & Davis, 2007; Bell & Zamudio, 2012; Ancillotto *et al.*, 2022; Mühlenhaupt *et al.*, 2025). In
99 anurans, these differences can either appear dynamically for the duration of the breeding season,
100 or can develop ontogenetically and persist across adult life, sometimes being detectable already
101 in juveniles (Hirschmann & Hödl, 2006; Sztatecsny *et al.*, 2010; Bell & Zamudio, 2012;
102 Ujhegyi & Bókony, 2020; Höbel *et al.*, 2022). In contrast to anurans with conspicuous
103 aposematic colouration (Rojas, 2017), the dorsal appearance of ‘true frogs’ (genus *Rana*) is
104 usually brownish, which may facilitate camouflage via background matching on leaf litter
105 (Barnett *et al.*, 2021; Rojas *et al.*, 2023). Nevertheless, sexual dichromatism occurs in this genus
106 too. Adult males of the moor frog (*R. arvalis*) undergo dynamic colour change from brown to
107 conspicuous blue for the breeding season. The function of blueness is subject to debate, but it
108 might either facilitate mating success or serve male recognition (Hettyey *et al.*, 2009b;
109 Sztatecsny *et al.*, 2012). In the wood frog (*R. sylvatica*), males feature somewhat greener dorsal
110 colouration compared to females already as juveniles (Lambert *et al.*, 2017). In various anurans,
111 including nocturnal species, conspicuous throat coloration (underside of the head) and
112 coloration of the anterior trunk may provide important cues for mating (Gomez *et al.*, 2009;
113 Höbel *et al.*, 2022; Robertson *et al.*, 2022). In the common frog (*R. temporaria*), sexual
114 dichromatism only became apparent to researchers when they observed animals in their natural
115 breeding habitat during night time (Sztatecsny *et al.*, 2010). Under these circumstances, the
116 throat of common frog males appeared bright whitish in contrast to the darker reddish throats
117 of females. Dorsal colouration of agile frogs can vary along a broad range of brown, yellow and
118 grey shades, and the underside features limited pigmentation that taxonomic guides describe as
119 white (or pink) without any characteristic patterns (AmphibiaWeb, 2026). Nevertheless, some
120 ventral pigmentation can be detected (Fig S1). Despite being a widespread species in Europe,
121 no systematic assessment of sexual dichromatism in agile frogs has been attempted to our
122 knowledge.

123 If colouration in agile frogs, similarly to other *Rana* species plays a role in male recognition,
124 then detectable colouration differences between sex-reversed ‘XX males’ and concordant ‘XY

125 males' could be key for females to differentiate between males with different genotypes. With
126 other words, colouration might contribute to the decreased siring success of 'XX males' in the
127 wild (Bókonyi *et al.*, 2025b). In this study we had two goals. First, we tested whether adult
128 female, sex-reversed 'XX male' and concordant 'XY male' agile frogs differed in either dorsal
129 or ventral colouration during the breeding season. Second, we assessed whether the frog vision
130 model predicted differentiation among the three sex categories based on overall dorsal and
131 throat colouration. We measured the average red, green and blue reflectance for the dorsum and
132 for the throat, and calculated hue, saturation and brightness from these values. We used the
133 average reflectance values against the vision model of a related *Rana* species for which
134 information was retrievable. Additionally, handling several hundred frogs, we noticed greater
135 variation in two types of ventral patterns distinguishable by the human eye (i.e. symmetrically
136 distributed red patterns, and dark pigmentation along the mouth). We recorded these features
137 for each individual and assessed whether the sexes differed in them.

138

139 **2. Methods**

140 **2.1. Animal collection and sexing**

141 The agile frog breeding season in our study region (Hungary, Central Europe) starts in late
142 February or early March, and lasts until late March or early April, depending on the weather
143 conditions. We collected free-ranging adults at arrival for breeding from pitfall traps around a
144 fenced breeding pond near Budapest (47.551195°N, 18.926682°E) in February-March 2024
145 and transported them to our nearby (ca. 700 m) experimental station in Julianna-major at the
146 Plant Protection Institute. Each frog was photographed and released into the pond within 24
147 hours after falling into a pitfall trap (see section 2.2. for details on photography). The animals
148 were weighed on a digital scale with ± 0.01 g accuracy.

149 We used established methods to determine the phenotypic and the genotypic sex of each
150 individual. Male phenotype was determined by the presence of nuptial pads, and female
151 phenotype was recognized based on large belly size (i.e. filled with eggs). For genotypic sexing,
152 we collected buccal swabs and used E.Z.N.A. Forensic DNA Kit (Omega Bio-Tek, Inc.) to
153 extract DNA following the manufacturer's protocol. We used sex-linked genotypic sex markers
154 following the established agile frog sexing protocol (Nemesházi *et al.*, 2020). In short, we
155 screened all individuals for the Rds3 marker using high-resolution melt analysis (HRM) and, in
156 cases of mismatch between genotype and phenotypic sex, we amplified the Rds1 locus with

157 PCR to confirm sex reversal. Only the unambiguously genotyped males were included in this
158 study. Based on nearly 10 years of research, agile frog females always feature the XX genotype
159 (i.e. no XY females were ever detected; Nemesházi *et al.*, 2020; Bókony *et al.*, 2021; Mikó *et*
160 *al.*, 2021), and we therefore deemed it unnecessary to determine the genotype of each female.
161 Based on combined information on genotypic and phenotypic sex, we classified each individual
162 as female, ‘XY male’, or ‘XX male’ (i.e. sex-reversed). Hereafter, we will refer to this combined
163 information of genotypic and phenotypic sex as consensus sex.

164 **2.2. Photography and colouration**

165 We took dorsal photos of all individuals, and ventral photos of a subset of the individuals (see
166 details in the next paragraph; examples are shown in Fig S2). Photos were taken under standard
167 lighting conditions provided by a 5000K LED light (Matcheasy Banda LED 5V-U-3-5K). High-
168 resolution raw images (CR3; 24.2 MP) were captured with a Canon EOS R50 digital camera
169 (Canon Inc.) that was mounted on a tripod. Aiming to minimise glare on the frog skin, we
170 equipped the camera with a circular polarization filter (Hoya UX II slim frame, 49mm). We
171 operated the camera using the Canon Camera Connect smart phone application (version
172 3.0.10.23; Canon Inc.). We photographed a ColorChecker Classic mini card (X-Rite Inc.;
173 hereafter colour standard) each day and each time when the camera was re-mounted on the
174 tripod (e.g. due to battery change), approximately at the same spot where the animals were
175 photographed. Our dataset contained no more than one ventral and one dorsal photo per
176 individual, as ensured by photo-based individual identification (Nemesházi *et al.*, 2026). We
177 had ventral photos for only a subset of the captured individuals, and we excluded from our
178 dataset all photos that did not provide a view of the vast majority of the throat area. In practice,
179 ca. up-to the size of a frog finger was accepted to obscure the throat, which was left out from
180 the area selected for colour measurement. Furthermore, we excluded all photos showing lesions
181 (e.g. blisters) on the frog’s skin that could have potentially biased colouration measurements.

182 We measured average dorsal and throat colouration on the digital photographs in the
183 Multispectral Image Calibration and Analysis toolbox (MICA) version 2.2.3 (Troscianko &
184 Stevens, 2015) plugin in ImageJ version 1.54g (Schneider *et al.*, 2012). A single image was
185 analysed per individual (see Fig S2 for examples). We had 45 dorsal and 27 ventral images of
186 ‘XX males’. To obtain equal representation of each combination of sexual phenotypes and
187 genotypes, we randomly chose the same numbers of images (one per individual) featuring
188 females and ‘XY males’ as well, resulting in a total of 135 dorsal and 81 ventral images used
189 for these measurements. We opened the raw image files with the ‘generate multispectral image’

190 function in MICA, calibrated them with the black, grey and white tiles of the colour standard
191 (reference greyscale values were taken from Figure 2 in Gaiani *et al.*, 2017), and created a
192 ‘linear normalized reflectance stack’ from each image. We manually selected the region of
193 interest (ROI): the back area following the ridges that frame the dorsum of agile frogs (on dorsal
194 photos), or the approximate throat area denoted by the lower jaw (on ventral photos). For each
195 ROI, we extracted reflectance values in the RGB colour space, corresponding to the visible
196 spectrum: red (R; ~600 to 700 nm), green (G; ~500 to 600 nm) and blue (B; ~400 to 500 nm).
197 Based on these values, we calculated hue (the dominant wavelength; i.e. green, yellow, red
198 etc.), saturation (the intensity of the colour), and brightness (the amount of light reflected; often
199 denoted by V for ‘value’) according to the HSV colour space using the ‘rgb2hsv’ function of
200 the ‘grDevices’ package in R version 4.5.2 (R Core Team, 2025).

201 As our vision model approach, we used scotopic visual-space proxy model. Frog visual space
202 was estimated using a scotopic *Rana temporaria* proxy model to approximate low-light
203 perception in the focal system. Spectral sensitivity functions were reconstructed with the
204 Govardovskii visual-pigment template (Govardovskii *et al.*, 2000), parameterized to the two
205 rod classes reported for anuran vision, with peak sensitivities at approximately 430 nm and 502
206 nm (Sztatecsny *et al.*, 2010). This template-based reconstruction provides a standard,
207 biologically interpretable perspective to represent receptor sensitivity from known peak
208 wavelengths, while avoiding the stronger claim of direct physiological measurement.
209 Calibrated Mica RGB values were then transformed into estimated rod catches, yielding patch
210 values in a frog-relevant perceptual space rather than in camera-native colour coordinates.
211 Noteworthy, as the analysis is based on image-derived measurements (and not on full
212 reflectance spectra), it should be interpreted as an ecologically reasonable proxy: it is suited for
213 comparing relative differences among patches and sex classes under a shared calibration
214 framework, but it does not reconstruct absolute spectral properties of the skin or the full
215 complexity of frog colour vision. In that sense, the model provides a low-light approximation
216 for comparative sensory ecology analyses. To quantify perceptual separation under the low-
217 light visual proxy, we calculated just-noticeable differences (JNDs) from predicted rod catches
218 derived from calibrated Mica RGB values using the dichromat model.

219 To enable further measurements and manual assessment of specific human-visible features, we
220 processed one ventral photo per individual (of all individuals for which images were available)
221 in additional software (75 females, 27 ‘XX males’ and 105 ‘XY males’). After converting the
222 raw image files to DNG file format in Adobe DNG Converter version 15.4.0.1508 (Knoll *et al.*,

223 2023), we assigned a matching colour profile and the same pre-saved exposure curve to each
224 photo in RawTherapee version 5.9 (The RawTherapee Team, 2022). The colour profiles were
225 created from images of the colour standard in ColorChecker Camera Calibration version 2.2.0
226 (X-Rite Inc., 2020). We saved the colour-corrected ventral frog photos in jpeg format with the
227 ‘best quality’ option in RawTherapee. We opened these images in Fiji (running with ImageJ
228 version 1.54g; Schneider *et al.*, 2012), and measured the relative coverage of dark pigment
229 patterns on the ventral surface of the head, close to the tip of the mouth (hereafter referred to as
230 ‘chin mottling’) by our custom-developed plugins ‘frog chin selection’ and ‘mottling threshold’
231 (Supplement 1). First, we manually selected the area denoted by the mouth opening (Fig S3 A-
232 B). Then, in the ‘frog chin selection’ plugin we placed a point selection at the tip of the mouth,
233 after which the plugin automatically selected the ROI (Fig S3 C-E). Finally, we used the
234 ‘mottling threshold’ plugin to select those pixels which were darker than a pre-defined
235 threshold, calculate the area of dark patches (‘area%’) and create a masked image for
236 visualization (Fig S3 F). Further details on how the plugins were created, as well as a detailed
237 user guide are available in Supplement 1. In the ‘mottling threshold’ plugin, we used a pixel-
238 darkness threshold that could suitably capture the contrast between the pigment-based mottling
239 and the surrounding skin across our ventral photos, as determined based on 10 haphazardly
240 chosen images.

241 Capturing ventral images, we noticed the presence of roughly symmetrical red patterns (patches
242 and dots) on the throat and anterior part of the trunk of a considerable proportion of the
243 individuals (hereafter ‘red ventral pattern’; Fig S2 D). To assess whether this feature could be
244 sex-linked, one author (E.N.) categorized the extent of ‘red ventral pattern’ on each individual’s
245 photo on an ordinal scale using a photo guide (Fig S4) as follows: no red patterns at all (‘level
246 0’), animals with suspected but dubious presence of faint red patches or dots (‘level 1’), animals
247 on which some scattered red patches or dots were unambiguously present but did not form a
248 clear pattern (‘level 2’), and animals on which several red patches or dots formed clearly visible
249 pattern on the anterior part of the trunk and the throat (‘level 3’). Unavoidably, the sex of the
250 individuals could be detected by the observer on the photos. Although the observer deliberately
251 ignored sex when assigning the ‘red ventral pattern’ categories, we cannot exclude the
252 possibility that this information unconsciously affected the decisions. We could not crop the
253 images in a standard way that would provide a complete view of the area of interest while
254 excluding all potentially visible secondary sexual characteristics. First, the presence or absence
255 of nuptial pads would be visible on all photos where the animals held their front limbs partially

256 in front of the trunk or throat. Second, the dark pigmentation along the mouth can also provide
257 a clue about the sex of the animal (see the results on ‘chin mottling’). To validate that the
258 subjectively assigned ‘red ventral pattern’ categories also corresponded with objectively
259 measured differences (i.e. average throat colouration), we performed additional statistical
260 analyses as described in Supplement 2.

261 To make sure that the ‘red ventral pattern’ is not a peculiarity of our focal population, we
262 manually browsed several hundred agile frog observations available from across the species
263 range on the iNaturalist platform (<https://www.inaturalist.org/>). We focused on photos on which
264 the throat of the animal was visible, and the phenotypic sex could be determined based on the
265 presence of nuptial pads in males and either a large belly or visible eggs (if the animal was
266 found dead) in females. Additionally, we received a few photos of agile frogs of known
267 phenotypic sex taken by colleagues during their fieldwork. Altogether, we retrieved images of
268 22 phenotypic females and 14 phenotypic males with unambiguously determined sex. The
269 visibility of the anterior part of the trunk and throat greatly varied between these images,
270 preventing accurate quantification. Therefore, we report the presence or absence of the ‘red
271 ventral pattern’ as detected on the photos, without performing statistical analysis of these data.

272 **2.3. Statistical analyses**

273 Statistical analyses were performed in R 4.5.2 (R Core Team, 2025). As the main interest of
274 our study was to evaluate whether females, ‘XX males’ and ‘XY males’ differed from each
275 other in the measured features of colouration, first we performed models where the consensus
276 sex reflecting the genotype-phenotype combinations was the only predictor. We used linear
277 models with the ‘lm’ function for the hue, saturation and brightness variables, with two
278 exceptions. For ventral hue and ventral saturation, homoscedasticity was not met, so we used
279 generalized least squares model by the ‘gls’ function of the ‘nlme’ package (Pinheiro & Bates,
280 2025) to allow for group-specific variances (‘varIdent’ argument). We analysed the differences
281 between the consensus sex categories in the proportion of ‘chin mottling’ using beta distribution
282 with logit link using the ‘glmmTMB’ function of the ‘glmmTMB’ package (Brooks *et al.*,
283 2026). Because of heteroscedasticity, we allowed for different variances between sex categories
284 in the latter model too (‘dispformula’ argument). Additionally, we also performed a sensitivity
285 test for each model to assess whether the differences between sexes were robust enough to
286 persist when further potential predictors were included. As additional predictors, we used body
287 mass and day of arrival to the breeding pond (i.e. the day of the year at photo capturing).
288 Because females are larger than males, and males often arrive much earlier to the breeding pond

289 than females, to avoid multicollinearity, we centred both predictors by subtracting the mean of
290 the relevant phenotypic sex from the original value of each individual. Because sample
291 collection was not designed to enable assessing the effects of these additional predictors,
292 interactions were not included in the sensitivity tests. For every model, we used the ‘emmeans’
293 function of the ‘emmeans’ package (Lenth & Piaskowski, 2026) to calculate pairwise contrasts
294 between the consensus sex categories, and we applied Benjamini-Hochberg false discovery rate
295 (FDR) correction for the 3 p-values from each model (Pike, 2011). Model diagnostics were
296 performed for all models by the ‘simulateResiduals’ function of the ‘DHARMA’ package
297 (Hartig, 2024), whenever this was possible. Because ‘DHARMA’ is not suitable for the ‘gls’
298 models, for those we calculated model residuals and fitted values with the default R functions
299 called ‘resid’ and ‘fitted’, respectively, and visualized them by the ‘plot’ and ‘qqnorm’
300 functions for evaluation of model fitting.

301 We used linear models with the ‘lm’ function to test whether frog vision enabled differentiation
302 between the consensus sex categories based on either average dorsal or average ventral
303 colouration, respectively. JNDs were estimated from predicted rod catches using a
304 computational low-light visual proxy, and group differences were evaluated using bootstrapped
305 dichromat distance estimates.

306 The occurrence of the ‘level 3’ category of the ‘red ventral pattern’ variable was limited to one
307 consensus sex category, preventing us from finding a well-fitting model. Therefore, we applied
308 Kruskal-Wallis rank sum test using the ‘kruskal.test’ base function to evaluate whether females,
309 ‘XX males’ and ‘XY males’ significantly differed from one another in ‘red ventral pattern’. We
310 performed pairwise comparisons of the consensus sex categories by Mann-Whitney U tests with
311 the ‘wilcox.test’ function, and finally applied FDR correction for the p-values using the
312 ‘p.adjust’ function (‘stats’ package; R Core Team, 2025).

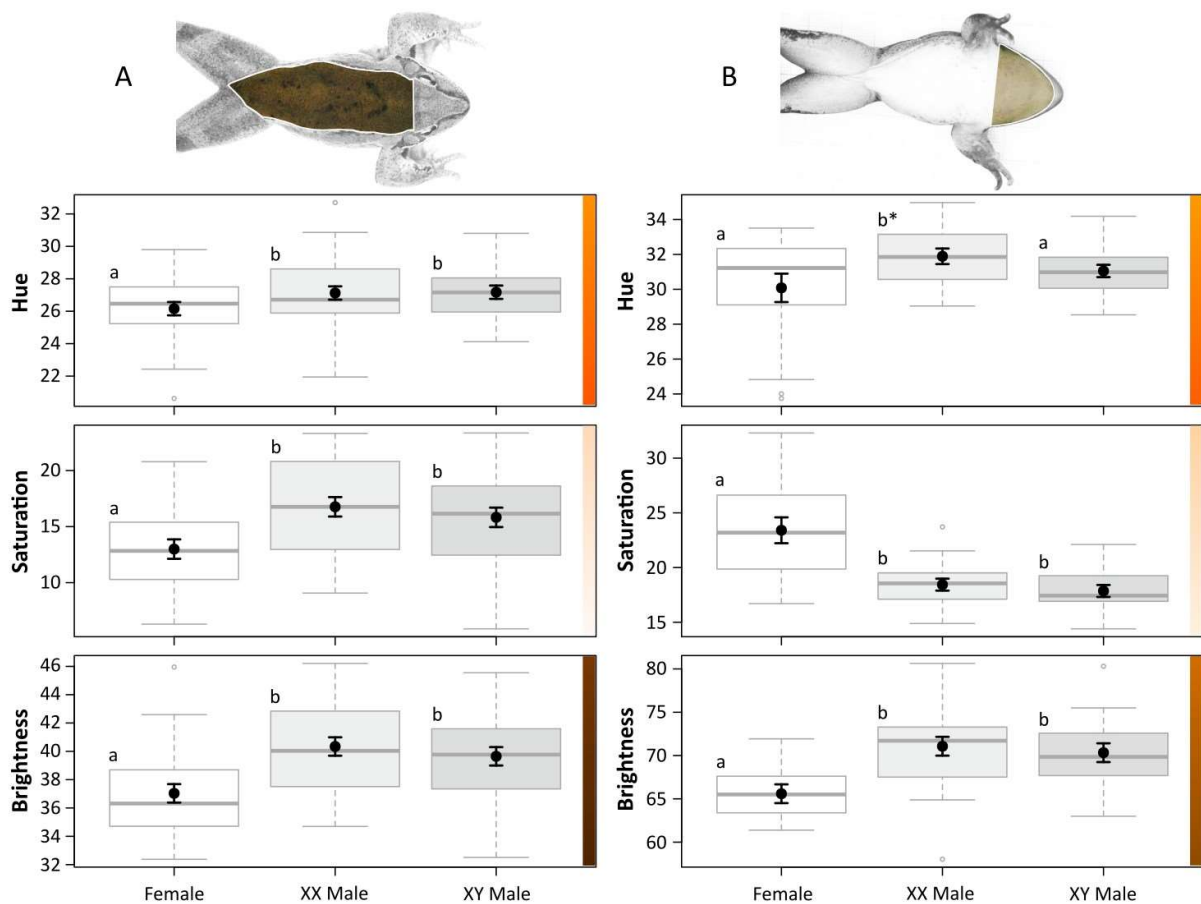
313 In all analyses, we used 95% confidence levels. For illustrative purposes, in the figures we
314 plotted mean estimates with 84% confidence intervals (CI) for each group, because non-
315 overlapping 84% CIs correspond approximately to statistical significance at $p < 0.05$ in pairwise
316 comparisons (Payton *et al.*, 2003).

317

318 **3. Results**

319 Regarding the average dorsal colouration, the main linear models revealed that females featured
 320 significantly more reddish colour (hue), lower saturation, and appeared overall darker (i.e.
 321 lower brightness) than both ‘XX males’ and ‘XY males’ (Fig 1 A; see detailed results in
 322 Supplement 3). ‘XX males’ did not differ from ‘XY males’ in any of these variables. The
 323 sensitivity tests confirmed that all these differences between females and ‘XX males’ as well
 324 as between females and ‘XY males’ were robust (remained significant; Supplement 3).

325



326

327 **Fig 1. Average dorsal (A) and throat (B) hue, saturation and brightness.** Colour bars on the
 328 right illustrate human-visible differences along the corresponding Y axis. Letters at the top of
 329 the boxes indicate statistically significant differences within each model (groups with different
 330 letters differ at $P < 0.05$ after FDR correction). The only exception is the letter marked with
 331 asterisk on panel B, where the FDR-corrected P-value for the ‘XX M’ vs. ‘XY M’ comparison
 332 was marginally nonsignificant ($p = 0.0566$; note that the corresponding p-value was 0.026 in
 333 the sensitivity test). Black dots represent model-estimated marginal means, and black error bars
 334 indicate 84% confidence intervals. In each boxplot, the median is denoted by the thick grey
 335 line, the interquartile range (IQR) is shown by the box, $IQR \pm 1.5 \times IQR$ is denoted by grey

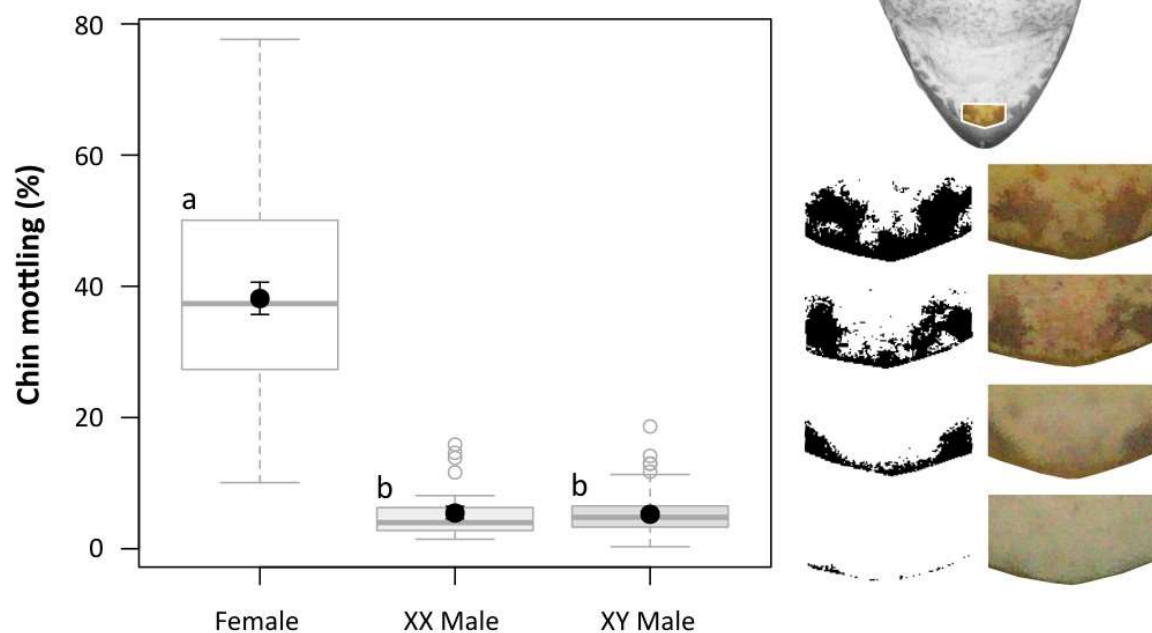
336 whiskers, and data points more extreme than these latter values are represented by empty
337 circles.

338 The average throat colouration in females was significantly darker (lower brightness) and more
339 saturated compared to both 'XX males' and 'XY males' (Fig 1 B; see detailed results in
340 Supplement 3). The sensitivity tests confirmed that these differences were robust (Supplement
341 3). The throat of 'XX males' had was relatively more yellowish (statistically significant
342 difference in hue) compared to females, and somewhat also compared to 'XY males', but the
343 latter was just above the significance threshold ($P = 0.0566$) after FDR correction. However,
344 this latter difference became significant ($p = 0.026$) when body mass and arrival date were also
345 considered in the model (Supplement 3).

346 The vision model suggested that the frog vision system is likely able to detect the average
347 differences in dorsal and ventral colouration between females and males regardless of their
348 genotypes (Supplement 4). By comparison, the divergence between 'XX males' and 'XY
349 males' was small and likely below the threshold of reliable discrimination (Supplement 4).

350 The proportion of 'chin mottling' was significantly larger in females compared to both 'XY
351 males' and 'XX males', whereas 'XX males' did not differ from 'XY males' according to the
352 main model (beta regression with logit link; see Fig 2 and detailed results in Supplement 2).
353 Results of the sensitivity test were qualitatively the same (Supplement 2)

354



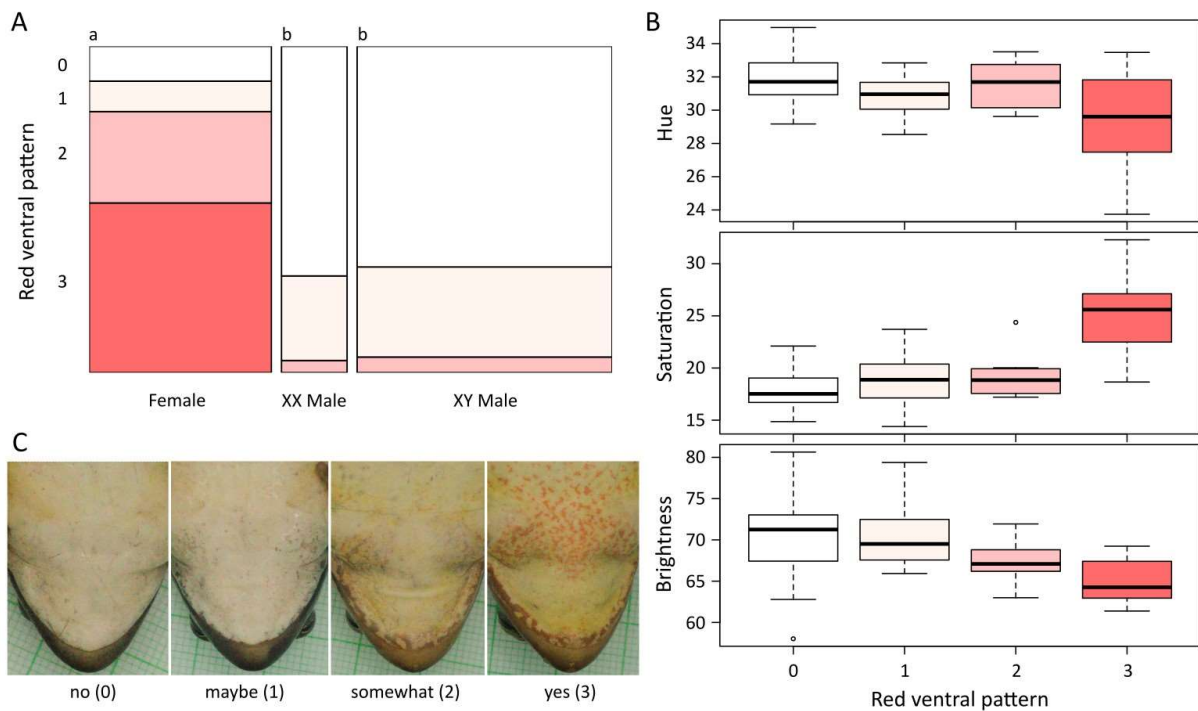
355

356 **Fig 2. Percentage of dark ventral pigmentation near the frontal middle part of the mouth**
357 **(‘chin mottling’)**. Example images on the right illustrate the masked view (saved in Fiji) and
358 the original view on frogs with varying ‘chin mottling’ proportions (from bottom to top: 1.5,
359 20.3, 40.5 and 59.4%, respectively). The ROI is denoted on the head photo on top. Letters on
360 the top of the boxes indicate statistically significant differences within each plot (groups with
361 different letters differ at $P < 0.05$ after FDR correction). Black dots and error bars, respectively,
362 represent estimated marginal means and 84% confidence intervals, both back-transformed from
363 the logit scale to the original percentage scale. See Fig 1 for the interpretation of box plots.

364

365 The Kruskal-Wallis test revealed that females significantly differed from both ‘XY males’ and
366 ‘XX males’ in the occurrence of the ‘red ventral pattern’ while there was no difference between
367 ‘XX males’ and ‘XY males’ (Fig 3 A; see detailed results in Supplement 2). The ‘level 3’
368 category, representing an unambiguous red patterning, was unique to females and it occurred
369 in 52% of them (Fig 3 A). The subjectively assigned ‘red ventral pattern’ categories
370 corresponded with differences in objectively measured average throat colouration (see Fig 3 B
371 and the Supplement 2) and coincided with decreasing throat brightness from ‘level 0’ to ‘level
372 3’. Additionally, the throat of animals with the ‘level 3’ category featured much higher average
373 saturation, as well as overall more reddish colour compared to all other individuals (Fig 3 B).
374 Animals in the ‘level 2’ category also tended to have relatively higher saturation (Fig 3 B).

375 Based on the images obtained from outside the study population (Table S1), the ‘red ventral
376 pattern’ was present in at least 18 out of the 22 females (‘level 3’ in 16 individuals, and ‘level
377 2’ in two individuals). For the remaining four females, throat visibility did not allow a confident
378 categorization based on the photos. Throat visibility allowed for the categorization of 12 out of
379 the 14 males. Among these, no sign of the ‘red ventral pattern’ was detected in 11 males (‘level
380 0’), and it was present at limited extent (‘level 2’) in a single male. The females for which
381 categorization was possible were photographed in seven different countries (Austria, Croatia,
382 France, Greece, Hungary, Italy and Ukraine). The male observations came from five countries
383 (Austria, France, Hungary, Italy and Slovakia). Three photos of females and two photos of
384 males were taken during autumn, while all others were taken during spring, around the breeding
385 season. During autumn, all three females had ‘level 3’ ‘red ventral pattern’, and one of the two
386 males was the only male with some ‘red ventral pattern’ (‘level 2’) detected in this dataset.



387

388 **Fig 3. Distribution of the ‘red ventral pattern’ categories in females, ‘XX males’ and ‘XY**
 389 **males’ (A), and the relationships of these ordinal categories with the average colouration**
 390 **of the throat (B).** The photos show one example per category (C). Small letters on the top of
 391 the mosaic plots (A) indicate statistically significant differences (groups with different letters
 392 differ at $P < 0.05$ after FDR correction).

393

394 4. Discussion

395 The agile frog is conventionally assumed to have a white ventral colouration without pigment
 396 patterns and features of interest (AmphibiaWeb, 2026). However, our study revealed sexual
 397 dichromatism in breeding adults that is visible by the human eye: phenotypic males and females
 398 significantly differed in average saturation and brightness of the throat area, the percentage of
 399 ‘chin mottling’ and the presence and extent of ‘red ventral pattern’. Furthermore, in line with
 400 the frog vision model, males and females appear to be distinguishable from one another on the
 401 basis of their average dorsal and average throat colour.

402 Agile frog males keep territories and use advertisement calls to attract females when breeding
 403 density is low (Lesbarrères *et al.*, 2008), but when breeding density is high (which is often the
 404 case, including the focal breeding pond of our study), they engage in scramble competition
 405 (Hettyey *et al.*, 2014). Female agile frogs can enforce their mate preferences when being

406 clasped by either conspecific or heterospecific males (Hettyey *et al.*, 2009a; Vági & Hettyey,
407 2016; Bókony *et al.*, 2025b). First, they can refuse to lay eggs for a long period, while a more
408 suitable partner might replace the male momentarily clasping them. Second, they can lay a
409 subset of their eggs for the unwanted male, encouraging it to end the amplexus, and potentially
410 giving opportunity to a more desirable partner to fertilize the rest of the eggs. It is currently
411 unknown which male features females take into account for mate preference aside from certain
412 call characteristics (Lesbarrères *et al.*, 2008), but colouration is a reasonable candidate, as visual
413 communication can be key for successful breeding in various amphibians (Hirschmann & Hödl,
414 2006; Bell & Zamudio, 2012; Rojas, 2017; Höbel *et al.*, 2022; Rojas *et al.*, 2023). Despite being
415 fertile, sex-reversed ‘XX males’ have lower breeding success compared to concordant ‘XY
416 males’ in the wild, and females tend to lay their eggs in two portions more often when paired
417 with ‘XX males’ (Bókony *et al.*, 2025b). Based on reports on other frog species, the appearance
418 of the male throat might influence breeding success (Sztatecsny *et al.*, 2010; Höbel *et al.*, 2022),
419 and therefore females might potentially differentiate between males based on throat colouration.
420 The only feature in which ‘XX males’ appeared to differ from ‘XY males’ in our dataset was
421 the hue of the throat, that was somewhat skewed towards yellow compared to the relatively
422 redder hue the ‘XY males’. However, the visual modelling analysis suggested that this colour
423 difference would not be detectable under the applied computational low-light proxy, indicating
424 that throat coloration is unlikely to explain the reduced mating success of ‘XX males’ in agile
425 frogs. While ours is the first systematic assessment of the colouration of sex-reversed and
426 concordant individuals in an amphibian, differences in throat colouration among male
427 individuals has been previously speculated to reflect sex reversal in the green frog (*Lithobates*
428 *clamitans*; Stephenson & Christensen, 2023). This speculation is in accordance with our
429 findings in the agile frog.

430 Most of the females included in our study featured the ‘red ventral pattern’ to some extent,
431 while it was largely missing from males. Qualitative comparison of the images of adult agile
432 frogs from a broad geographical range also confirmed that the ‘red ventral pattern’ is a common
433 feature in this species, and that it occurs predominantly in females. It seems surprising that this
434 human-visible feature was overlooked by herpetologists so far. The simplest explanation is that
435 ventral colouration, as in other amphibians as well, received much less attention compared to
436 dorsal colouration that is far more apparent from the human eye view (Plewnia *et al.*, 2024).
437 Alternatively, it is also possible that researchers who noticed the presence of the ‘red ventral
438 pattern’ assumed that it was a symptom of a disease instead of a potentially sex-linked feature,

439 due to its dubious appearance. We did not perform histological analysis and therefore cannot
440 exclude the possibility that the ‘red ventral pattern’ was caused by skin lesions. However, we
441 are unaware of any infectious amphibian disease that cause symmetrical skin lesions restricted
442 to the frontal half of the ventral surface of the body, or that cause symptoms largely restricted
443 to one sex (Chai, 2015; Pessier, 2018). Colour and patterns on the skin of vertebrates are
444 produced by the combination of different cell types and pigments (Rojas *et al.*, 2023). Red
445 colouration, for instance, can be produced by certain carotenoids, and sometimes even by
446 haemoglobin (Mills & Patterson, 2009). Therefore, taking the currently available data together,
447 the ‘red ventral pattern’ is most likely a normal feature of agile frog colouration. This pattern
448 is largely missing in adult males, that in turn feature a much brighter throat. Similar sexual
449 dichromatism was reported in common frogs, where breeding males also featured bright whitish
450 throat compared to the dark reddish throat of females (Sztatecsny *et al.*, 2010). This species
451 was observed to engage in heterospecific amplexus with agile frogs in shared breeding ponds,
452 despite the fact that they do not hybridize (Hettyey *et al.*, 2014). Similarly to what was
453 hypothesised for the common frog (Sztatecsny *et al.*, 2010), the bright throat of agile frog males
454 might facilitate sex recognition and decrease the probability that (conspecific) males would
455 mistakenly engage in amplexus with one another. Misdirected amplexus is a widespread
456 phenomenon which can have negative consequences on the fitness of both participants (i.e.
457 missing out on actual breeding opportunities; Mollov *et al.*, 2010; Vági & Hettyey, 2016;
458 Serrano *et al.*, 2022; Brischoux & Lorrain-Soligon, 2024). Furthermore, in rarer cases,
459 amplexus may even lead to the death of the clasped individual (Mollov *et al.*, 2010), although
460 conspecific males normally respond to release calls by stopping the amplexus (Marco & Lizana,
461 2002). Alternatively, presence or absence of a ‘red ventral pattern’ might also affect male fitness
462 if female agile frogs rely to some extent on throat colouration for mate preference. In line with
463 the logic of any of the above hypotheses, the lack of ‘chin mottling’ in males might also increase
464 fitness by enlarging the conspicuously bright surface on the throat. However, we are not aware
465 of studies assessing sex-linked differences in pigmentation along the mouth of amphibians, and
466 on the potential function of such patterns.

467 In conclusion, colouration may play a role in conspecific communication in the agile frog, and
468 our study took the first step towards exploring this aspect of evolution in an amphibian with
469 thermal sex reversal. We found differences between males and females in several aspects of
470 colouration, and even found subtle difference between sex-reversed and concordant males in
471 average throat hue. However, because this difference is not detectable within the limits of the

472 applied frog-vision proxy, we believe that throat coloration alone is unlikely to explain the
473 observed limited breeding success of sex-reversed males.

474

475 **Acknowledgements**

476 We are grateful to Mihály Balázs Ruzs for his help in developing the Fiji plugins, to Emese
477 Balogh, Victoria Oberreiter-Moritz and Nadine Lehofer for contributing to the DNA
478 extractions, and to Szilvia Kalogeropoulou for helping with literature search on diseases that
479 cause skin lesions in amphibians as well as consulting further veterinarians about this topic. We
480 thank Dávid Herczeg, Boglárka Kovács and Karina Smole-Wiener for giving us access to
481 ventral photos that they captured on the field. Infrastructure for DNA laboratory works was
482 provided by the Genetics Lab of the Konrad Lorenz Institute of Ethology of the University of
483 Veterinary Medicine Vienna, the VetCore Lab of the University of Veterinary Medicine Vienna
484 (Austria), and the laboratory of the Molecular Ecology Group of the University of Veterinary
485 Medicine Budapest (Hungary). This research was funded in part by the Austrian Science Fund
486 (FWF) [grant ESP 239-B to E.N.]. For open access purposes, the author has applied a CC BY
487 public copyright license to any author-accepted manuscript version arising from this
488 submission. Part of the funding came from the National Research, Development and Innovation
489 Office of Hungary (K-135016); during data analysis and manuscript writing V.B. was supported
490 by Project no. ADVANCED 152228 implemented with the support provided by the Ministry
491 of Culture and Innovation of Hungary from the National Research, Development and
492 Innovation Fund, financed under the National Research Excellence Program ADVANCED_25
493 subprogram funding scheme. A.K. was supported by the ÚNKP-23-4 New National Excellence
494 Program of the Ministry for Innovation and Technology from the source of the National
495 Research, Development and Innovation Fund (ÚNKP-23-4-I-ELTE-128). Z.M. was supported
496 by the EKÖP-24 University Excellence Scholarship Program of the Ministry for Culture and
497 Innovation from the source of the National Research, Development and Innovation Fund, and
498 by the National Research, Development and Innovation Office of Hungary (PD-134241). N.U.
499 was supported by 'SEH Grant in Herpetology' and the EKÖP-MATE/2025/26/K university
500 research Scholarship Program of the Ministry for Culture and Innovation from the source of the
501 National Research, Development and Innovation Fund. The funders had no role in study design,
502 data collection and analysis, decision to publish, or preparation of the manuscript.

503

504 **AI usage**

505 The ‘frog chin selection’ Fiji plugin was built with the assistance of ChatGPT (version GPT-4)
506 and it was manually corrected for syntax errors. The R code used for vision model extraction
507 was implemented using GPT-5.4-codex.

508

509 **Supporting information**

510 The dataset, as well as supplementary figures, supplementary information on the methods and
511 results and R codes are available in FigShare at [https://doi.org/ 10.6084/m9.figshare.31647649](https://doi.org/10.6084/m9.figshare.31647649).

512

513

514 **References**

515 AmphibiaWeb. 2026. <<https://amphibiaweb.org>> University of California, Berkeley, CA,
516 USA. Accessed 30 Mar 2026.

517 Ancillotto, L., Vignoli, L., Martino, J., Paoletti, C., Romano, A. & Bruni, G. 2022. Sexual
518 dichromatism and throat display in spectacled salamanders: a role in visual
519 communication? *J. Zool.* **318**: 75–83.

520 Barnett, J.B., Michalis, C., Scott-Samuel, N.E. & Cuthill, I.C. 2021. Colour pattern variation
521 forms local background matching camouflage in a leaf-mimicking toad. *J. Evol. Biol.* **34**:
522 1531–1540.

523 Baroiller, J.F. & D’Cotta, H. 2001. Environment and sex determination in farmed fish. *Comp.*
524 *Biochem. Physiol. - C Toxicol. Pharmacol.* **130**: 399–409.

525 Bell, R.C. & Zamudio, K.R. 2012. Sexual dichromatism in frogs: natural selection, sexual
526 selection and unexpected diversity. *Proc. R. Soc. B* **279**: 4687–4693.

527 Bókony, V., Balogh, E., Mikó, Z., Kásler, A., Örkényi, Z. & Ujhegyi, N. 2025a. Higher sex-
528 reversal rate of urban frogs in a common-garden experiment suggests adaptive
529 microevolution. *Evol. Appl.* **18**: e70093.

530 Bókony, V., Balogh, E., Ujhegyi, N., Mikó, Z., Kásler, A., Ujszegi, J., *et al.* 2025b. Complex
531 effects of sex reversal on reproductive success in wild frogs.

532 Bókony, V., Ujhegyi, N., Mikó, Z., Erös, R., Hettyey, A., Vili, N., *et al.* 2021. Sex reversal
533 and performance in fitness-related traits during early life in agile frogs. *Front. Ecol.*
534 *Evol.* **9**: 745752.

535 Brischoux, F. & Lorrain-Soligon, L. 2024. Anuran swingers: misdirected mating attempts
536 occurred early during anuran diversification. *Biol. J. Linn. Soc.* **141**: 529–536.

537 Brooks, M., Bolker, B., Kristensen, K., Maechler, M., Magnusson, A., Skaug, H., *et al.* 2026.
538 glmmTMB: Generalized Linear Mixed Models using Template Model Builder. Version:
539 1.1.14.

540 Chai, N. 2015. Anurans. In: *Fowler's Zoo and Wild Animal Medicine, Volume 8* (R. E. Miller
541 & M. E. Fowler, eds), pp. 1–13. Elsevier.

542 Edmunds, J.S.G., McCarthy, R.A. & Ramsdell, J.S. 2000. Permanent and functional male-to-
543 female sex reversal in d-rR strain medaka (*Oryzias latipes*) following egg microinjection
544 of o,p'-DDT. *Environ. Health Perspect.* **108**: 219–224.

545 Gaiani, M., Apollonio, F., Ballabeni, A. & Remondino, F. 2017. Securing color fidelity in 3D
546 architectural heritage scenarios. *Sensors* **17**: 2437.

547 Geffroy, B. & Wedekind, C. 2020. Effects of global warming on sex ratios in fishes. *J. Fish*
548 *Biol.* **97**: 596–606.

549 Gomez, D., Richardson, C., Lengagne, T., Plenet, S., Joly, P., Léna, J.P., *et al.* 2009. The role
550 of nocturnal vision in mate choice: Females prefer conspicuous males in the European
551 tree frog (*Hyla arborea*). *Proc. R. Soc. B Biol. Sci.* **276**: 2351–2358.

552 Govardovskii, V.I., Fyhrquist, N., Reuter, T., Kuzmin, D.G. & Donner, K. 2000. In search of
553 the visual pigment template. *Vis. Neurosci.* **17**: 509–528.

554 Hartig, F. 2024. DHARMA: Residual Diagnostics for Hierarchical (Multi-Level / Mixed)
555 Regression Models. Version: 0.4.7.

556 Hettyey, A., Baksay, S., Vági, B. & Hoi, H. 2009a. Counterstrategies by female frogs to
557 sexual coercion by heterospecifics. *Anim. Behav.* **78**: 1365–1372.

558 Hettyey, A., Herczeg, G., Laurila, A., Crochet, P.A. & Merilä, J. 2009b. Body temperature,
559 size, nuptial colouration and mating success in male Moor Frogs (*Rana arvalis*). *Amphib.*
560 *Reptil.* **30**: 37–43.

561 Hettyey, A., Vági, B., Kovács, T., Ujszegi, J., Katona, P., Szederkényi, M., *et al.* 2014.
562 Reproductive interference between *Rana dalmatina* and *Rana temporaria* affects
563 reproductive success in natural populations. *Oecologia* **176**: 457–464.

564 Hirschmann, W. & Hödl, W. 2006. Visual signaling in *Phrynobatrachus krefftii* Boulenger,
565 1909 (Anura: Ranidae). *Herpetologica* **62**: 18–27.

566 Höbel, G., Feagles, O. & Ruder, E. 2022. Diversity and sexual dichromatism in treefrog throat
567 coloration: Potential signal function? *J. Herpetol.* **56**: 294–301.

568 Knoll, T., Chan, E., Bury, J., Castleberry, C., Castro, K., Chen, S., *et al.* 2023. *Adobe DNG*
569 *Converter version 15.4.0.1508. Accessed from*
570 *https://www.adobe.com/go/dng_converter_win.*

571 Lambert, M.R., Carlson, B.E., Smylie, M.S. & Swierk, L. 2017. Ontogeny of sexual
572 dichromatism in the explosively breeding wood frog. *Herpetol. Conserv. Biol.* **12**: 447–
573 456.

574 Lande, R., Seehausen, O. & van Alphen, J.J.M. 2001. Mechanisms of rapid sympatric
575 speciation by sex reversal and sexual selection in cichlid fish. *Genetica* **112–113**: 435–
576 443.

577 Lenth, R. V & Piaskowski, J. 2026. emmeans: Estimated Marginal Means, aka Least-Squares
578 Means. Version: 2.0.2.

579 Lesbarrères, D., Merilä, J. & Lodé, T. 2008. Male breeding success is predicted by call
580 frequency in a territorial species, the agile frog (*Rana dalmatina*). *Can. J. Zool.* **86**:
581 1273–1279.

582 Li, H., Holleley, C.E., Elphick, M., Georges, A. & Shine, R. 2016. The behavioural
583 consequences of sex reversal in dragons. *Proc. R. Soc. B Biol. Sci.* **283**: 1–7.

584 Marco, A. & Lizana, M. 2002. The absence of species and sex recognition during mate search
585 by male common toads, *Bufo bufo*. *Ethol. Ecol. Evol.* **14**: 1–8.

586 Mikó, Z., Nemesházi, E., Ujhegyi, N., Verebélyi, V., Ujszegi, J., Kásler, A., *et al.* 2021. Sex
587 reversal and ontogeny under climate change and chemical pollution: are there
588 interactions between the effects of elevated temperature and a xenoestrogen on early
589 development in agile frogs? *Environ. Pollut.* **285**: 117464.

- 590 Mills, M.G. & Patterson, L.B. 2009. Not just black and white: Pigment pattern development
591 and evolution in vertebrates. *Semin. Cell Dev. Biol.* **20**: 72–81.
- 592 Mollov, I.A., Popgeorgiev, G.S., Naumov, B.Y., Tzankov, N.D. & Stoyanov, A.Y. 2010.
593 Cases of abnormal amplexus in anurans (Amphibia: Anura) from Bulgaria and Greece.
594 *Biharean Biol.* **4**: 121–125.
- 595 Mühlenhaupt, M., Hey, R., Starp, M., Anthes, N., Bachhausen, P., Bamann, T., *et al.* 2025.
596 Citizen science data reveals widespread sexual dichromatism in the European fire
597 salamander (*Salamandra salamandra*). *BMC Ecol. Evol.* **25**.
- 598 Nemesházi, E. & Bókony, V. 2023. HerpSexDet: the herpetological database of sex
599 determination and sex reversal. *Sci. Data* **10**: 377.
- 600 Nemesházi, E. & Bókony, V. 2025. Interplay of genotypic and thermal effects on sex
601 determination shapes climatic distribution in herpetofauna. *Glob. Ecol. Biogeogr.* **36**:
602 e70096.
- 603 Nemesházi, E., Gál, Z., Ujhegyi, N., Verebélyi, V., Mikó, Z., Üveges, B., *et al.* 2020. Novel
604 genetic sex markers reveal high frequency of sex reversal in wild populations of the agile
605 frog (*Rana dalmatina*) associated with anthropogenic land use. *Mol. Ecol.* **29**: 3607–
606 3621.
- 607 Nemesházi, E., Kövér, S. & Bókony, V. 2021. Evolutionary and demographic consequences
608 of temperature-induced masculinization under climate warming: the effects of mate
609 choice. *BMC Ecol. Evol.* **21**: 16. BioMed Central.
- 610 Nemesházi, E., Mikó, Z., Ujhegyi, N., Kásler, A., Lehofer, N. & Bókony, V. 2026. Placing
611 anurans in water can improve photo-based individual identification. *PLoS One* **21**:
612 e0341460.
- 613 Payton, M.E., Greenstone, M.H. & Schenker, N. 2003. Overlapping confidence intervals or
614 standard error intervals: What do they mean in terms of statistical significance? *J. Insect*
615 *Sci.* **3**: 1–6.
- 616 Pessier, A.P. 2018. Amphibia. In: *Pathology of Wildlife and Zoo Animals* (K. A. Terio, D.
617 McAloose, & J. St. Leger, eds), pp. 921–951. ElsevierAcademic Press.
- 618 Pike, N. 2011. Using false discovery rates for multiple comparisons in ecology and evolution.
619 *Methods Ecol. Evol.* **2**: 278–282.

620 Pinheiro, J. & Bates, D. 2025. nlme: Linear and Nonlinear Mixed Effects Models. Version:
621 3.1-168.

622 Plewnia, A., Lötters, S., Gomides, S., De Agrò, M. & Röbber, D.C. 2024. Sex-specific ventral
623 dichromatism and melanization in harlequin toads (*Atelopus*): a common but overlooked
624 character of unknown function. *Evol. Ecol.* **38**: 571–583.

625 R Core Team. 2025. *R: A language and environment for statistical computing*. R ver. 4.5.2. R
626 Foundation for Statistical Computing, Vienna, Austria. <http://www.r-project.org>.

627 Robertson, J.M., Bell, R.C. & Loew, E.R. 2022. Vision in dim light and the evolution of color
628 pattern in a crepuscular/nocturnal frog. *Evol. Ecol.* **36**: 355–371. Springer International
629 Publishing.

630 Rojas, B. 2017. Behavioural, ecological, and evolutionary aspects of diversity in frog colour
631 patterns. *Biol. Rev.* **92**: 1059–1080.

632 Rojas, B., Lawrence, J. & Márquez, R. 2023. Amphibian coloration: Proximate mechanisms,
633 function, and evolution. In: *Evolutionary Ecology of Amphibians* (G. Moreno-Rueda &
634 M. Comas, eds), pp. 219–258. CRC Press, Boca Raton.

635 Schneider, C.A., Rasband, W.S. & Eliceiri, K.W. 2012. NIH Image to ImageJ: 25 years of
636 image analysis. *Nat. Methods* **9**: 671–675.

637 Serrano, F.C., Díaz-Ricaurte, J.C. & Martins, M. 2022. Finding love in a hopeless place: A
638 global database of misdirected amplexus in anurans. *Ecology* **103**: 2021–2022.

639 Stephenson, B.P. & Christensen, J. 2023. The relationship of body colouration to
640 morphological traits in a population of green frogs from Georgia, USA. *Amphibia-
641 Reptilia* **44**: 495–508.

642 Sztatecsny, M., Preininger, D., Freudmann, A., Loretto, M.-C., Maier, F. & Hödl, W. 2012.
643 Don't get the blues: conspicuous nuptial colouration of male moor frogs (*Rana arvalis*)
644 supports visual mate recognition during scramble competition in large breeding
645 aggregations. *Behav. Ecol. Sociobiol.* **66**: 1587–1593.

646 Sztatecsny, M., Strondl, C., Baierl, A., Ries, C. & Hödl, W. 2010. Chin up: are the bright
647 throats of male common frogs a condition-independent visual cue? *Anim. Behav.* **79**:
648 779–786.

649 The RawTherapee Team. 2022. RawTherapee 5.9. Accessed from <https://rawtherapee.com/>.

650 Todd, B.D. & Davis, A.K. 2007. Sexual dichromatism in the marbled salamander,
651 *Ambystoma opacum*. *Can. J. Zool.* **85**: 1008–1013.

652 Troscianko, J. & Stevens, M. 2015. Image calibration and analysis toolbox - a free software
653 suite for objectively measuring reflectance, colour and pattern. *Methods Ecol. Evol.* **6**:
654 1320–1331.

655 Ujhegyi, N. & Bókonyi, V. 2020. Skin coloration as a possible non-invasive marker for
656 skewed sex ratios and gonadal abnormalities in immature common toads (*Bufo bufo*).
657 *Ecol. Indic.* **113**: 106175. Elsevier.

658 Ujszegi, J., Bertalan, R., Ujhegyi, N., Verebélyi, V., Nemesházi, E., Mikó, Z., *et al.* 2022.
659 “Heat waves” experienced during larval life have species-specific consequences on life-
660 history traits and sexual development in anuran amphibians. *Sci. Total Environ.* **835**:
661 155297.

662 Vági, B. & Hettyey, A. 2016. Intraspecific and interspecific competition for mates: *Rana*
663 *temporaria* males are effective satyrs of *Rana dalmatina* females. *Behav. Ecol.*
664 *Sociobiol.* **70**: 1477–1484. Behavioral Ecology and Sociobiology.

665 Whiteley, S.L., Castelli, M.A., Dissanayake, D.S.B., Holleley, C.E. & Georges, A. 2021.
666 Temperature-induced sex reversal in reptiles: prevalence, discovery, and evolutionary
667 implications. *Sex. Dev.*, doi: 10.1159/000515687.

668 Wild, K.H., Roe, J.H., Schwanz, L., Rodgers, E., Dissanayake, D.S.B., Georges, A., *et al.*
669 2023. Metabolic consequences of sex reversal in two lizard species: a test of the like-
670 genotype and like-phenotype hypotheses. *J. Exp. Biol.* **226**: jeb245657.

671 X-Rite Inc. 2020. *ColorChecker Camera Calibration version 2.2.0*. Accessed from
672 <https://my.xrite.com/downloader.aspx?FileID=2215&Type=P>. X-Rite, Michigan USA.

673